

Fig 2: Cu accumulation curves in columns of Dowex 50x4 (100-200 mesh) resin, corresponding to samples containing the same (nominal) total Cu concentration and varying amounts of ligands forming neutral complexes. Panel a: complexes with R_{acc} equal to that of a solution in absence of ligand (at all recorded exposure times). Panel b: complexes with initial R_{acc} (at short exposure times) equal to that of a solution in absence of ligand, but diverging for longer times. Panel c: complexes with R_{acc} smaller than that of the solution in absence of ligand (i.e. just Cu). Panel d: complexes that equilibrate almost instantaneously with the resin. In each case, the accumulation curve in absence of ligands is shown for comparison purposes. Parameters: $m_{\text{resin}}=100$ mg; flow rate, $Q=4.5$ mL min^{-1} ; $c_{\text{T,Cu}}\approx 2.5\times 10^{-7}$ mol L^{-1} . See Table 3 for composition details. The dotted lines in panels b and c are a guide to the eye.

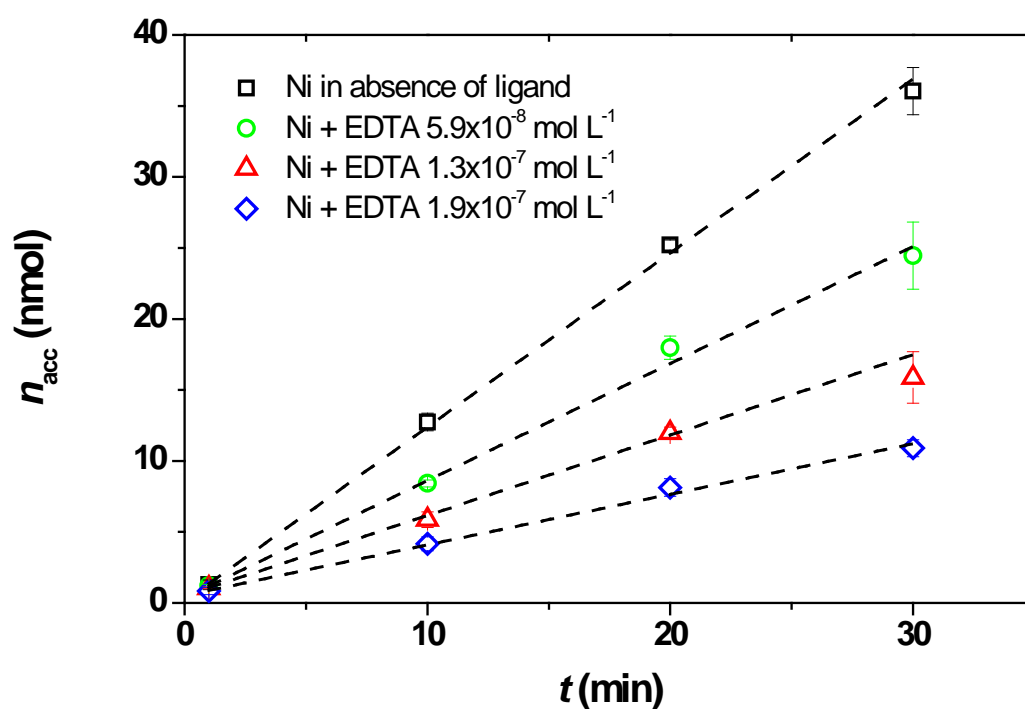


Fig 3: Accumulation curves of Ni in Dowex 50x4 (200-400 mesh) in presence of three different concentrations of EDTA exhibiting accumulation rates proportional to the free ion concentration. Each series corresponds to a different c_{Ni} , reported in the legend. The points stand for the average of three independent columns, while the dashed lines were given by the linear regression over all the data points $c_{T,Ni}=2.5 \times 10^{-7}$ mol L⁻¹, $Q=4.5$ mL min⁻¹.

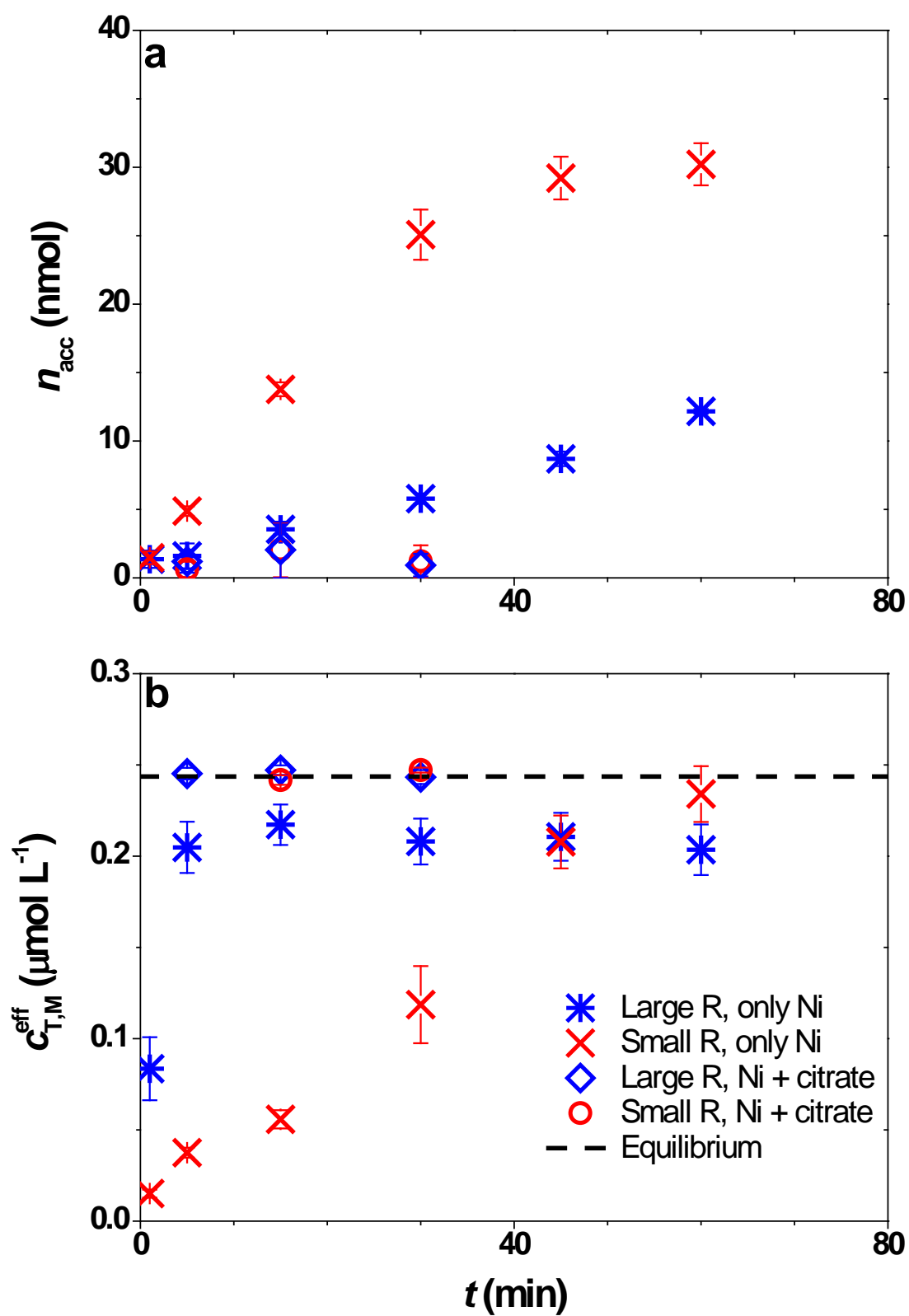


Fig 4: Accumulation of Ni, in presence and in absence of a competing ligand (citrate) on Dowex resin beads of different sizes ("large R": Dowex 50x8 50-100 mesh; "small R": Dowex 50x2 200-400 mesh). Panel a: accumulation curves; Panel b: breakthrough curves. Blue stars: no ligand added, resin 50-100 Mesh; red crosses: no ligand added, resin 200-400 Mesh; blue diamonds: citrate 5×10^{-4} mol L⁻¹, resin 50-100 Mesh; red circles: citrate 5×10^{-4} mol L⁻¹, resin 200-400 Mesh. In panel b the dashed line stands for the eventual equilibrium value. The experiments in absence of ligand were performed in triplicate, while the experiments in presence of citrate were performed in duplicate. In this latter case, the error bars are hidden by the symbols.

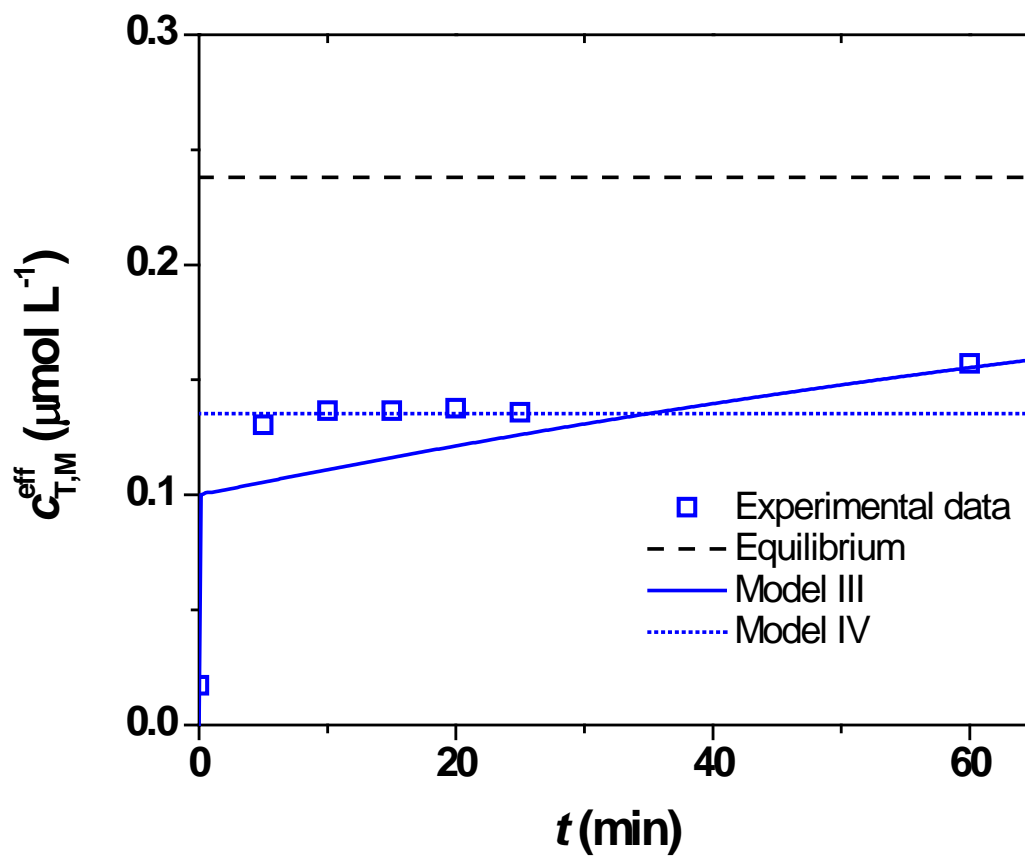


Fig 5: Breakthrough curve of Cu in presence of IDA, with $c_{T,IDA}=5\times 10^{-7}$ mol L⁻¹. Markers: experimental data; continuous blue line: Model III; dotted blue line: Model IV; dashed black line: equilibrium value. $c_{T,Cu}=2.47\times 10^{-7}$ mol L⁻¹, $Q=4.5$ mL min⁻¹.

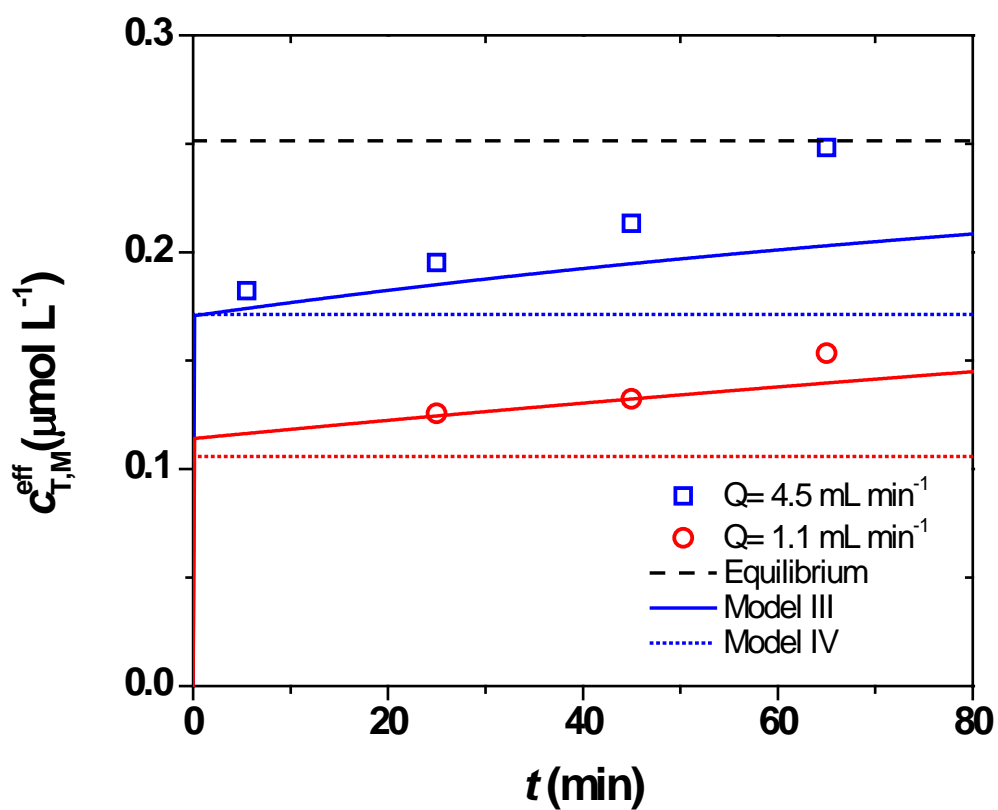


Fig 6: Impact of flow rate on breakthrough curves of Cu in absence of ligand, with $c_{T,M} = 2.5 \times 10^{-7} \text{ mol L}^{-1}$, $Q = 4.5$ (blue) and 1.1 (red) mL min^{-1} . Markers: experimental data; continuous lines: Model III; dotted lines: Model IV; dashed black line: equilibrium value.